

Synthesis and Steady-State Spectroscopic Study of 5-Aryl-2,2′-bipyridyls. New Fluorescent Compounds in Solid State

Naoko Mizuyama,[1] Yoshinori Tominaga,*[1] Shinya Kohra,[1] Kazuo Ueda,[1] Shun-ichi Hirayama,[2] and Yasuhiro Shigemitsu[3]

[1]Faculty of Environmental Studies, Nagasaki University, 1-14 Bunkyo-machi, Nagasaki 852-8521

[2]Sasebo National College of Technology, 1-1 Okishin-machi, Sasebo 857-1193

[3]Industrial Technology Center of Nagasaki, 2-1303-8 Ikeda, Omura 856-0026

Received August 16, 2005; E-mail: ytomi@net.nagasaki-u.ac.jp

The absorption and fluorescent properties of newly synthesized 5-aryl-2,2′-bipyridyls were examined both in solution and in the solid state. The 6-methoxy derivatives **5a**–**5c** have weak fluorescence, whereas 6-amino derivatives **7a**–**7f** showed strong fluorescence. Their spectroscopic properties were computationally analyzed using semi-empirical molecular orbital calculations. The geometries of the ground (S_0) and the first singlet excitation states (S_1) were optimized and employed to estimate the vertical transition energies. The drastic differences in fluorescent intensities between **5a**–**5c** and **7a**–**7f** can be qualitatively explained by the relative energy levels S_1 and the neighboring triplet level; the energy gaps supposedly regulate the non-radiative intersystem crossing (ISC) probabilities. On the relaxed S_1 geometry, **5a**–**5c** have quite small S_1–triplet energy gaps, whereas **7a**–**7f** have no such quasi-degeneracies, leading to their quantitatively different quantum yields.

The increasing attention to luminescent heterocycles has been driven by their industrial applications to a variety of organic light-emitting devices such as laser dyes,[1] electroluminescent materials,[2] biological probes,[3] and multiple other usage.[4] In the past few years, many fluorescent heterocyclic compounds have been synthesized: dicyanopyrazine derivatives,[5,6] bisazomethine dyes,[7] carbazole-based dyads,[8] and α-pyrones.[9] At the same time, a number of quantum chemical calculations have been reported to theoretically clarify the structure–spectroscopic property relationship of functional dyes[10–12] and to establish the reliable design of luminescent compounds.[13,14]

2,2′-Bipyridyls have been extensively utilized as chelating reagents to effectively form complexes with various metals.[15] However, few of them have been reported to serve as luminescent materials.[16] We herein apply the synthetic scheme reported by Potts et al.[17] to obtain novel fluorescent bipyridyls by using ketene dithioacetals, which have been found useful as active reagents.[18] We also report the UV–vis and fluorescence properties both in solution and in the solid state, the X-ray structural analysis, and the computational studies of the novel 5-aryl-2,2′-bipyridyls, mainly focusing on 6-methoxy-5-aryl-2,2′-bipyridyls (**5a**–**5f**, weakly fluorescent) and 6-amino-5-aryl-2,2′-bipyridyls (**7a**–**7c**, strongly fluorescent). This sharp contrast in their fluorescent efficiency is a focal point to be discussed from the viewpoints of their structural and electronic characteristics.

Results and Discussion

Synthesis. The well-known Hantzsch synthesis, involving two molecules of β-ketone and one each of aldehyde and ammonia, is an important synthetic method of pyridines and polyarylpyridines. In line with the framework, α-oxo ketene dithioacetal and β-keto aldehydes have been used as three-carbon components to give (4-methylthio)pyridines in excellent yields. Although the use of ketene dithioacetals for the synthesis of 6-arylbipyridyls is well known,[17] the synthesis of 6-hydroxy-, 6-methoxy-, and 6-amino-5-aryldipyridyls bearing an aryl group at the 5-position of a bipyridyl ring has not been reported.

The whole synthetic scheme in this study is described in Fig. 1. The reaction of 3,3-dimethylthio-1-(2-pyridyl)prop-2-en-1-one (**1**) with phenylacetonitrile (**2a**) in the presence of powdered sodium hydroxide in dimethyl sulfoxide (DMSO), followed by treatment with water gave 4-methylthio-5-phenyl-6-oxo-1*H*-2,2′-bipyridyl (**4a**) in 46% yield via the intermediate **3a**. The other 6-methoxy derivatives **4b** and **4c** were also prepared from **1**, **2b**, and **2c** in the same manner. Using methanol instead of water, this treatment gave the corresponding 6-methoxy-2,2′-bipyridyls **5a**–**5c** in 54, 34, and 41% yields, respectively. Synthesis of the 6-aminobipyridyls **7a**–**7f** was realized using the strong nucleophilicity of amines. The reaction of **1** with **2a** in the presence of powdered sodium hydroxide in DMSO at room temperature smoothly gave the expected 4-methylthio-5-phenyl-6-(1-pyrrolidinyl)-2,2′-bipyridyl (**7a**) by treatment with pyrrolidine **6a** in 50% yield, via the intermediate **3a**. The other 1-pyrrolidinyl derivatives **7e** and **7f** were also obtained via **3b** and **3c** treated with pyrrolidine in 65 and 74% yields, respectively. **7b**–**7d** were obtained by the reaction of **3b** and **3c** with ammonium hydroxide and dimethylamine in 30, 40, and 60% yields, respectively.

Spectroscopic Measurement. The spectroscopic properties of **4a**–**4c**, **5a**–**5c**, and **7a**–**7f** were examined both in ethanol (in dichloromethane for **7a**, **7e**, and **7f**) and in the powdered form (Fig. 2). The results are summarized in Table 1. The first

Published on the web April 7, 2006; DOI: 10.1246/bcsj.79.602

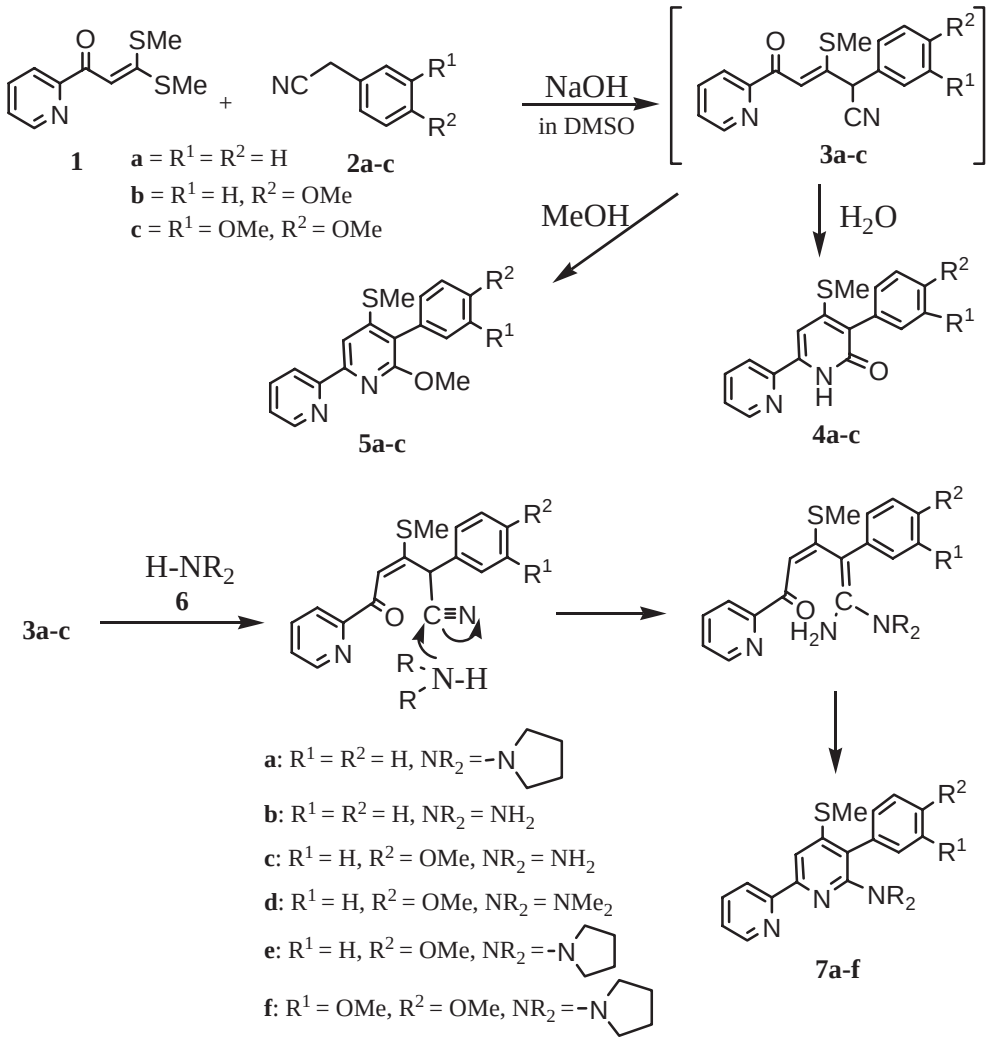

Fig. 1. Synthetic scheme of novel aryl-2,2′-bipyridyls **4a**–**4c**, **5a**–**5c**, and **7a**–**7f**.

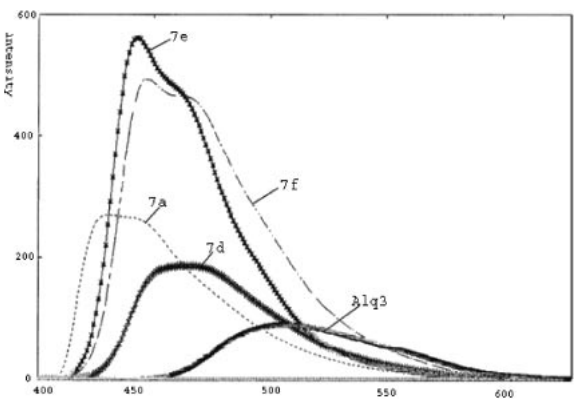

Fig. 2. Fluorescence spectra of **7a**, **7d**, **7e**, and **7f** and Alq3 in powdered state.

intense absorption maxima of **7a**–**7f** lie in a significantly longer wavelength region compared with those of **5a**–**5c** in ethanol. The fluorescence excitation maxima (not UV–vis absorption maxima) of **5a**–**5c** in ethanol bathochromically shifted from those in powdered form. In contrast, those of **7a**–**7f** showed a hypsochromic shift. For example, **5a** has an excitation peak at 284 nm in ethanol and at 354 nm in the solid state, whereas **7a** has the peak at 366 nm in ethanol and at 301 nm in the powdered state. This opposite phenomena indicates that the molecular packing field works oppositely for **5a**–**5c** and **7a**–**7f**; **5a**–**5c** are stabilized, whereas **7a**–**7f** are destabilized in the crystalline state.

The fluorescence maxima of **5a**–**5c** and **7a**–**7f** in ethanol ranged within 430–460 nm. The fluorescence quantum yields (QYs) were calibrated with anthracene (0.30 in ethanol) as a standard sample. The QYs of **5a**–**5c** were found to be quite small (0.01–0.03), whereas **7a**–**7f** possess significantly larger QYs. In particular, **7a**, **7e**, and **7f** with a pyrrolidiono group showed intense fluorescence. The small QYs of **7b** could be explained by an amino–imino tautomerism associated with the excited state intramolecular proton transfer (ESIPT), which contributes to the efficient radiationless deactivation. **5a**–**5c** showed significantly larger Stokes shifts (SS) than **7a**–**7f**, indicating the more stabilized S_1 states of **5a**–**5c** than **7a**–**7f** in the solvent polarization field. Meanwhile, the QYs of **7a**, **7e**, and **7f** measured in dichloromethane drastically dropped (ca. 0.01), indicating the heavy atom effects of dichloromethane or the solvent effects, which may affect the relative singlet/triplet energy levels of the molecules. **7f** showed a larger red shift

Table 1. UV–Vis and Fluorescence Spectra of **4a–4c**, **5a–5c**, and **7a–7f** in Ethanol, CH_2Cl_2, and in Powdered State

Entry	In solution (ethanol, CH_2Cl_2)						Powdered state			
	λ_{max} /nm	(log ε)	Ex[a] /nm	Em[a] /nm	SS[b]	QY[c]	Ex /nm	Em /nm	SS[d]	RI[e]
4a	354	(4.07)	353	430	64	0.02	344	479	35	2.12
4b	314	(4.16)	359	475	116	0.13	345	482	127	2.96
4c	369	(4.14)	360	504	144	0.07	349	469	110	2.41
5a	307	(4.34)	284	436	152 (79)	0.01> (0.01>)	354	482	128	0.27
5b	310	(4.33)	290	443	153	0.03	359	429	70	0.60
5c	310	(4.32)	288	458	170	0.01>	360	484	127	0.54
7a	355	(4.06)	366	444	78	0.31	301	431	130	2.18
7b	330	(4.23)	333	432	66	0.15	319	510	91	0.16
7c	343	(4.24)	323	434	111	0.25	307	407	100	1.21
7d	349	(4.10)	336	452	116	0.17	301	466	165	4.50
7e	357	(4.27)	345	447	102 (102)	0.35 (0.01>)	300	442	142	6.81
7f	358	(4.03)	349	453	104 (61)	0.32 (<0.01)	300	459	159	7.84
Alq3							341	510	169	1.00

a) Measured in ethanol. b) Stokes shift in ethanol and in CH_2Cl_2 (in parenthesis). c) Quantum yields as standard of anthracene (0.30 in ethanol). QY in parenthesis measured in CH_2Cl_2. d) Stokes shift in powdered state. e) Relative intensity of fluorescence in the powdered state as standard of Alq3.

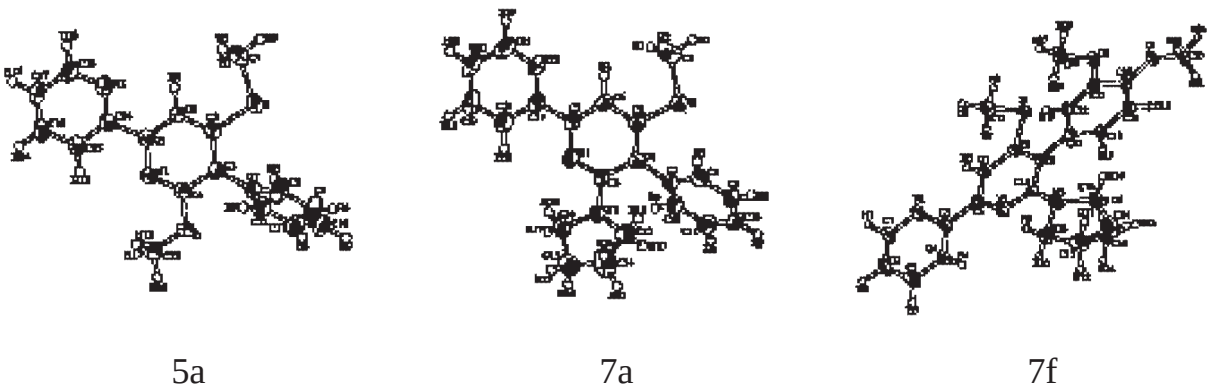

Fig. 3. ORTEP drawings of **5a**, **7a**, and **7f**.

of its emission peak (more than 70 nm) than **7a** and **7e**.

In powdered form, fluorescence relative intensities (R.I.) were measured with a standard of Alq3 (tris(8-hydroxyquinolinato)aluminium). **7a–7f** showed larger SS than **5a–5c**, opposite to the case in ethanol. The substitution effect on the fluorescence intensity showed sharp contrast between **5a–5c** and **7a–7f**. In the case of **7a–7f**, the R.I. was considerably enhanced by the introduction of a methoxy group to the aryl ring. Remarkably, strong fluorescence was observed for **7e** and **7f**, those of R.I. was 6.81 and 7.84 times stronger than Alq3, respectively. These figures are far larger than α-pyrones reported by Hirano et al.[9] In the case of **5a–5c**, however, no remarkable enhancement was observed by the introduction of a methoxy group on the aryl ring.

X-ray Crystallographic Study. X-ray crystallographic analysis was carried out for **5a**, **7a**, and **7f**. The ORTEP drawings and analytical data are shown in Fig. 3 and Table 2, respectively. For **5a**, the torsional angle between the two pyridine rings (θ) is 13 degrees and the dihedral angle between the aryl ring and the connecting pyridine ring (ϕ) is 71 degrees. Such a distorted geometry is qualitatively true for **7a** and **7f**; no major differences were found among their crystal structures with the aryl ring perpendicularly twisted from the molecular plane.

Table 2. Crystallographic Data of **5a**, **7a**, and **7f**

	5a	**7a**	**7f**
Empirical formula	$C_{18}H_{16}N_2OS$	$C_{21}H_{21}N_3S$	$C_{23}H_{25}N_3O_2S$
Fw	308.40	347.48	407.53
Color	clear	clear	yellow
Habit	block	block	block
Crystal system	orthorhombic	monoclinic	monoclinic
Space group	$P2_12_12_1$ (#19)	$P2_1/n$ (#14)	$P2_1/c$ (#14)
a/Å	8.789	5.6971	9.3982
b/Å	10.6351	19.222	11.166
c/Å	16.8883	16.6632	20.0194
β/deg		91.4901	101.2532
V/Å^3	1578.6	1824.2	2060.4
Z	4	4	4
R	0.050	0.074	0.065
R_w	0.076	0.111	0.126
$R1$	0.035	0.050	0.046

Hirano et al. reported a drastic variation between the fluorescent intensity of α-pyrones in powdered (crystal) state and in evaporated film (amorphous) state.[9] They claimed that

Table 3. Key Geometrical Parameters of **5a**, **7a**, and **7f** in the S_0 and S_1 States

Parameters	**5a**			**7a**			**7f**		
	S_0		S_1	S_0		S_1	S_0		S_1
	X-ray[a]	calc.[b]	calc.[b]	X-ray[a]	calc.[b]	calc.[b]	X-ray[a]	calc.[b]	calc.[b]
$r(N_1–C_4)$	1.32	1.36	1.34	1.34	1.37	1.36	1.34	1.35	1.35
$r(N_1–C_5)$	1.35	1.35	1.37	1.34	1.35	1.35	1.34	1.36	1.36
$r(C_2–C_3)$	1.40	1.41	1.42	1.40	1.42	1.42	1.40	1.40	1.41
$r(C_2–C_6)$	1.39	1.41	1.42	1.40	1.40	1.41	1.40	1.41	1.41
$r(C_3–C_4)$	1.40	1.43	1.44	1.42	1.43	1.44	1.42	1.43	1.44
$r(C_3–C_7)$	1.49	1.46	1.45	1.50	1.46	1.46	1.49	1.47	1.46
$r(C_5–C_6)$	1.38	1.41	1.40	1.38	1.41	1.41	1.39	1.40	1.40
$r(C_5–C_{14})$	1.48	1.49	1.49	1.49	1.49	1.49	1.49	1.49	1.49
$r(C_7–C_8)$	1.38	1.40	1.45	1.39	1.42	1.40	1.38	1.40	1.40
θ ($C_6–C_5–C_{14}–N_2$)	12.7	54.9	41.4	13.9	49.4	44.7	11.9	30.0	38.8
ϕ ($C_2–C_3–C_7–C_8$)	70.7	89.2	45.6	71.4	88.9	57.9	81.9	87.0	68.4

a) X-ray crystallographic data. b) AM1-SDCI(8,8) calculations.

strong fluorescence is observed in the powdered state, whose packing field hinders rotation of aryl rings whereas weak or no fluorescence is observed in the film state, which liberates the rotation freedom to open up a radiationless decay pathway. In our case, however, the weak fluorescent **5a** also holds the rotation-blocked structure as in the case of **7a**–**7f**. This means there are reasons other than the different magnitude of intermolecular steric hindrance between **5a**–**5c** and **7a**–**7f** to explain the drastic differences in their fluorescent intensities.

Computational Study

Computational Details. Quantum chemical calculations were performed using CAChe Worksystem program package version 5.04 for Windows.[19] Geometry optimizations for the S_0 and S_1 states were carried out employing the semi-empirical AM1 Hamiltonian[20] combined with the single and double excitation configuration interaction (SDCI) method where the 8 electrons were distributed within the 8 near-frontier orbitals to replicate the electron correlation effect lacked in the Hartree–Fock level of theory; this computational scheme is abbreviated by AM1-SDCI(8,8) hereafter. The accuracy of the AM1-CI technique has been established to give qualitatively trustworthy results in various cases involving photochemical processes.[21–23] The conformation analysis was carried out by varying the two key torsional degrees (θ, ϕ) by 30 degrees independently, with the other geometrical parameters optimized at each point. From the discrete points examined in the two-dimensional (θ, ϕ) surfaces, full geometry optimizations were performed in order to find the global minimum point which was in turn employed for the following spectral calculations.

The vertical transition energies and the associated properties (transition dipole moments, oscillator strengths, etc.) were computed within the framework of ZINDO with the INDO/1 Hamiltonian.[24] The Single CI space composed of the 9 highest occupied and the 9 lowest unoccupied orbitals generate 65 singly excited configurations, which is a default setting of the calculation. We preliminarily examined the influence of CI space for the computed λ_{max} and oscillator strengths, with a 14×14 Single CI calculation giving 197 configurations. As a result, we confirmed that the variation of the CI space slightly affects the calculation results in this study.

In both AM1-CDCI and ZINDO calculations, no solvent effects were taken into consideration.

Ground State Geometries and Absorption Peaks. The representative geometrical parameters of **5a**–**5c** and **7a**–**7f**, key dihedral angles (θ, ϕ) and bond lengths are summarized in Table 3. The **5a** optimal angles (θ, ϕ) are (55, 91), indicating the mutually twisted two pyridine rings and the perpendicular conformation of the aryl ring to minimize steric crowding. The calculated (θ, ϕ) were qualitatively consistent with those of crystallographic data. The qualitative agreement between theory and experiment is also true in the case of **7a** and **7f**.

Regarding the potential energy barriers, **5a** has the energy barrier of 8 kcal mol^{-1} against planarity of the aryl ring caused by the bulky central pyridyl ring. The rotational barrier of the pyridine ring was in contrast quite small, 2 kcal mol^{-1} toward planarity. The energy landscape against planarity was also calculated in the case of **7a**: 14 kcal mol^{-1} barrier of the aryl ring rotation and almost free rotation of the pyridyl ring (1 kcal mol^{-1}).

The agreement of the bond lengths is fairly excellent between the crystallographic data and the AM1-SDCI(8,8) results as a whole, within 0.04 Å. Both in the case of **5a** and **7a**, the two key bond lengths connecting the aromatic rings were optimized to be 1.46 Å (pyridyl–phenyl) and 1.49 Å (pyridyl–pyridyl), respectively. These figures reflect little π-conjugative nature along the long molecular axis (Fig. 4).

Moving on to the spectral characteristics, ZINDO calculations were carried out to theoretically evaluate the absorption maxima and the nature of transitions as summarized in Table 4. **5a** has two intense peaks at 246 and 307 nm in ethanol. The calculations showed that the first allowed transition is describable by the HOMO $\rightarrow$ LUMO π–π^* excitation with its transition dipole polarized along the *x*-axis (in-plane long axis). The HOMO and LUMO π-lobes resided locally on the central pyridyl ring with little intramolecular π-resonance nature. The agreement between the experimental $S_0 \rightarrow S_1$ peak and the theoretical one is fairly good, 307 and 297 nm, respectively. The second allowed transition is expressed by the HOMO $\rightarrow$ LUMO+1 π–π^* excitation with an oscillator strength of 0.37. The theoretical $S_0 \rightarrow S_6$ peak (246 nm) corresponds to the absorption peak at 245 nm. $S_0 \rightarrow S_2$ to $S_0 \rightarrow$

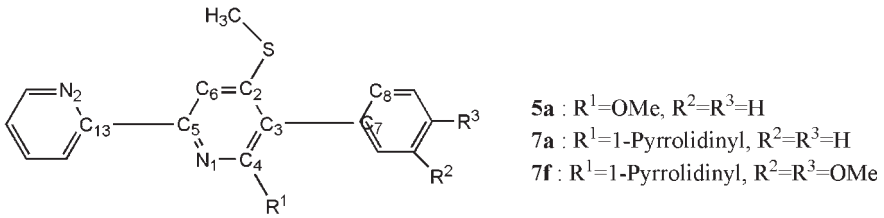

Fig. 4. Definition of atom numbers of **5a**, **7a**, and **7f**.

Table 4. Calculated $S_0 \rightarrow S_1$ Vertical Excitation Energies for **5a–5c** and **7a–7f** in the S_0 State

Entry	Transition character	MO coefficients of the main configuration[a)]	λ_{max} /nm	Oscillator strength	Polarization direction
5a	$\pi \rightarrow \pi^*$	H → L: 0.82	297	0.37	x
5b	$\pi \rightarrow \pi^*$	H → L: 0.81	302	0.51	x
5c	$\pi \rightarrow \pi^*$	H → L: 0.66, H → L+1: 0.49	300	0.48	x
7a	$\pi \rightarrow \pi^*$	H → L: 0.81	294	0.35	x
7b	$\pi \rightarrow \pi^*$	H → L: 0.83, H → L+1: 0.38	318	0.45	x
7c	$\pi \rightarrow \pi^*$	H → L: 0.83, H → L+1: 0.38	309	0.47	x
7d	$\pi \rightarrow \pi^*$	H → L: 0.80, H → L+1: 0.37	300	0.37	x
7e	$\pi \rightarrow \pi^*$	(H−1) → L: 0.75, H → L: 0.36	298	0.48	x
7f	$\pi \rightarrow \pi^*$	(H−1) → L: 0.56, H → L: 0.59	301	0.55	x

a) H: HOMO, L: LUMO.

S_5 peaks have negligibly small oscillator strengths.

For **7a**, the experimental peak appeared at 355 nm, at a longer wavelength region than **5a** by 48 nm. The calculation failed to reproduce this hypsochromic shift. The transition characters of the two main bands resembled those of **5a**.

Qualitative Assessment of ISC Probabilities. The drastic differences in the fluorescent intensities of α-pyrones were reported between in the powdered and in the thin film state, where the critical role of the packing field in the crystalline structure was pointed out to block free rotation of a 6-positioned aryl group.[9] This hypothesis, however, is unclear in whether it could be generalized to our case. The presence of substituents on the central pyridine ring of **5a–5c** and **7a–7f** severely interferes with the rotation of the aryl group. Actually, **7a–7f** have large quantum yields both in solution and in the solid state; in contrast, **5a–5c** show very weak emission in spite of their intramolecular sterically hindered structures. Their structural differences are just methoxy (**5a–5c**) and alkylamino (**7a–7f**) groups at the 6-position, and no significant geometrical deviation in the crystalline state between them, as indicated by both the X-ray structural analysis and quantum chemistry calculations previously mentioned. Thus, further rigorous explanations are required from the viewpoint of the differences in their electronic structures.

The well-known El-Sayed law,[25] which offers qualitative and intuitive insights into ISC probabilities, ensures efficient spin–orbit couplings with different excitation nature, such as between $^{1,3}(n,\pi^*)$ and $^{3,1}(\pi,\pi^*)$ states. On the other hand, small interactions exist between S–T coupling with the same excitation nature such as $^{1,3}(n,\pi^*)$–$^{3,1}(n,\pi^*)$ or $^{1,3}(\pi,\pi^*)$–$^{3,1}(\pi,\pi^*)$.

$$\left|\frac{\langle S(n,\pi^*)|H_{S.O.}|S(n,\pi^*)\rangle}{\langle S(\pi,\pi^*)|H_{S.O.}|S(n,\pi^*)\rangle}\right|^2 \leq 10^{-3} \text{ (in case of pyradine).} \quad (1)$$

The law is derived from the compensation of electron spin momentum inversion with orbital angular momentum variation during the electronic transition accompanied by spin-flipping (so-called "$p_x \rightarrow p_y$ effect"), which means an electron jump between two spatially orthogonal atomic orbitals to effectively give first-order spin–orbit coupling matrix elements.[26] A typical example is biacetyl, which has $S_1(\pi,\pi^*)$ and the neighboring $T(n,\pi^*)$ state, undergoing cascade radiationless decay initiated by efficient $S \rightarrow T$ ISC followed by backward $T \rightarrow S^*$ process, finally leading to $S^* \rightarrow S_0$ internal conversion.[27]

Hence, we have examined the $S_1(\pi,\pi^*)$ and the neighboring $T(n,\pi^*)$ energy levels as well as the associated molecular orbitals described in Fig. 5, Fig. 6, and Table 5.

In the case of **5a**, the energy level of $S_1(\pi,\pi^*)$ with the HOMO → LUMO excitation in nature is close enough to have strong interactions with the neighboring triplet states $T_{10}(n,\pi^*)$, whose main configurations are expressed by the HOMO−5 (or HOMO−6) to LUMO excitations. Efficient $S_1(\pi,\pi^*) \rightarrow T_{10}(n,\pi^*)$ ISC occurs where the electron hopping from nitrogen lone pairs of HOMO−5 (or HOMO−6) to HOMO localized on the central pyridine ring is accompanied by the spin flipping. Its schematic explanation is given in Fig. 7. Such near-degeneracies between the S_1 and the close triplet levels are also seen for **5b** and **5c**.

On the other hand, **7a** has a moderate energy gap of 0.09 eV between $S_1(\pi,\pi^*)$ and the neighboring $T_{10}(n,\pi^*)$, of which the main configuration is also expressed by the excitation from the two nitrogen lone pairs of HOMO−7 (or HOMO−6) to the localized π-orbital on the central pyridine ring of LUMO, leading the small interaction between $S_1(\pi,\pi^*)$ and $T_{10}(n,\pi^*)$ to open up a radiative pathway. Compared with **7b** and **7c**, the S_1–T gaps of **7a**, **7e**, and **7f** with a pyrrolidino group widen, resulting in significantly intense fluorescence in the solid state.

Conclusion

This work has presented an experimental and theoretical analysis of the novel fluorescent 5-aryl-2,2′-bipyridyls; synthesis, spectroscopic properties, X-ray structural analysis, and computational study mainly focused on 6-metoxy- (**5a**–**5c**) and 6-amino-5-aryl-2,2′-bipyridyls (**7a**–**7f**). Especially, **7e** and **7f** showed remarkably strong fluorescence both in solution and in the powdered state (nearly 8 times as strong as Alq3), whereas **5a**–**5c** showed very weak fluorescence in both states.

X-ray structural analysis has revealed that **5a**, **7a**, and **7f** share an aryl ring conformation nearly perpendicular against the bipyridyl plane. These structures were also supported by the AM1-CISD(8,8) calculations. The intense fluorescence of **7a**–**7f** is supposedly caused by the rotational hindrance of the aryl ring, which blocks radiationless decay paths such as vibrational energy transfer. Actually, the aryl ring of **7a**–**7f** has the large rotation barrier of 14 kcal mol^{-1} in the ground state according to the MO calculations. In contrast to strongly fluorescent **7a**–**7f**, rigorous explanations are required for the weak fluorescence of **5a**–**5c**, which also hold severe rotation hindrance of the aryl ring as in the case of **7a**–**7f**. Our theoretical analysis claims that the weak fluorescence of **5a**–**5c** could be attributed to their electronic nature, i.e., the relative positioning of S_1 and the neighboring triplet state which regulates the ISC probabilities. The ZINDO calculations indicated that **5a**–**5c** have the quasi-degeneracies between the $S_1(\pi,\pi^*)$ and the neighboring triplet level $T_{10}(n,\pi^*)$. This situation is suitable for the efficient ISC between the two states which lead to their small fluorescent quantum yields. On the other hand, **7a**–**7f** have no such near-degeneracies and significantly strong fluorescence is observed.

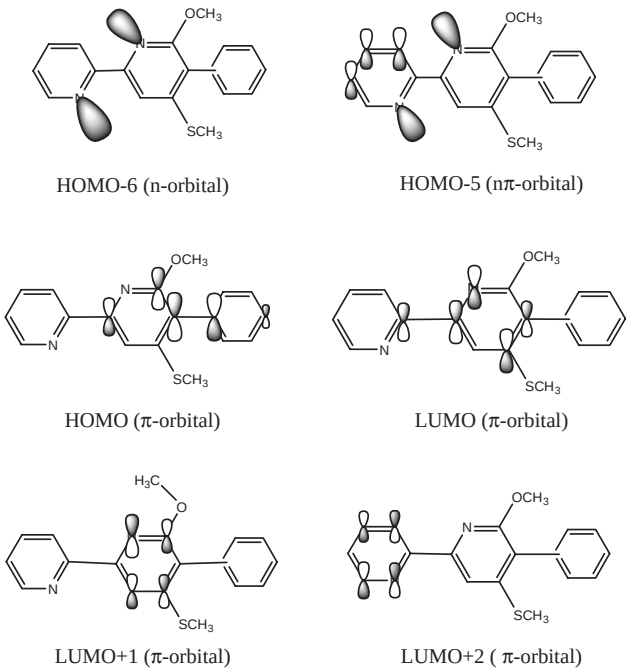

Fig. 5. Key molecular orbitals of **5a** in the S_1 optimized geometry.

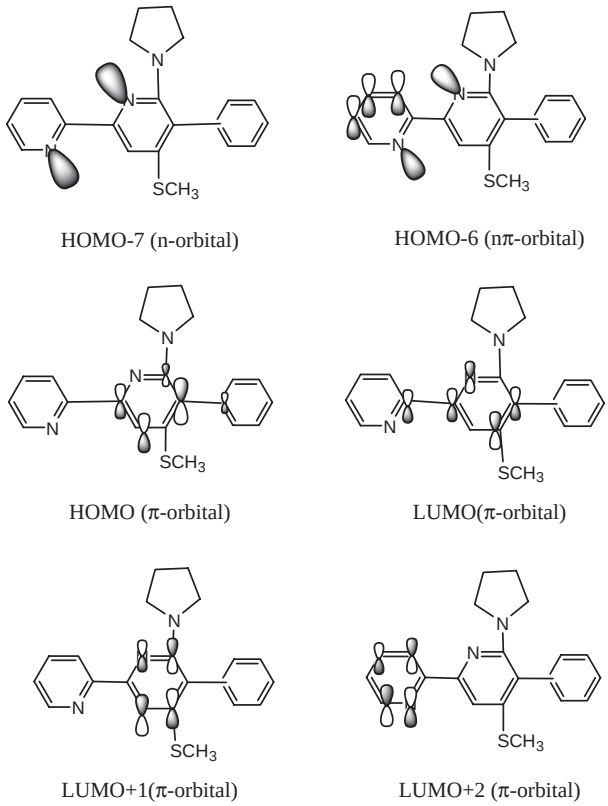

Fig. 6. Key molecular orbitals of **7a** in the S_1 optimized geometry.

Table 5. ISC Relevant Singlet/Triplet Energy Levels in the S_1 Optimized States of **5a**–**5c** and **7a**–**7f**

Entry	T[a]		S_1	
	Energy /(number of levels)	Character[b]	Energy	Character[b]
5a	3.87 (T_9)	n(H−6) → π^*(L) 0.17, n(H−5) → π^*(L) 0.36	3.87	π(H) → π^*(L) 0.82
5b	3.93 (T_9)	n(H−6) → π^*(L) 0.19, n(H−5) → π^*(L) 0.35	3.86	π(H) → π^*(L) 0.86
5c	3.93 (T_9)	n(H−6) → π^*(L) 0.31, π(H−5) → π^*(L) 0.37	3.91	π(H) → π^*(L) 0.65
7a	3.98 (T_9)	n(H−7) → π^*(L) 0.32, n(H−6) → π^*(L) 0.33	4.07	π(H) → π^*(L) 0.74
7b	3.90 (T_{10})	n(H−6) → π^*(L) 0.11, n(H−5) → π^*(L) 0.31	3.99	π(H) → π^*(L) 0.75
7c	3.90 (T_9)	n(H−6) → π^*(L) 0.51, n(H−5) → π^*(L) 0.03	3.96	π(H) → π^*(L) 0.82
7d	3.96 (T_9)	n(H−7) → π^*(L) 0.33, n(H−6) → π^*(L) 0.31	4.03	π(H) → π^*(L) 0.77
7e	3.96 (T_9)	n(H−7) → π^*(L) 0.29, π(H−6) → π^*(L) 0.37	4.13	π(H) → π^*(L) 0.71
7f	3.96 (T_9)	n(H−7) → π^*(L) 0.28, π(H−6) → π^*(L) 0.38	4.12	π(H) → π^*(L) 0.69

a) Neighboring triplet state to the S_1 state. b) H: HOMO, L: LUMO.

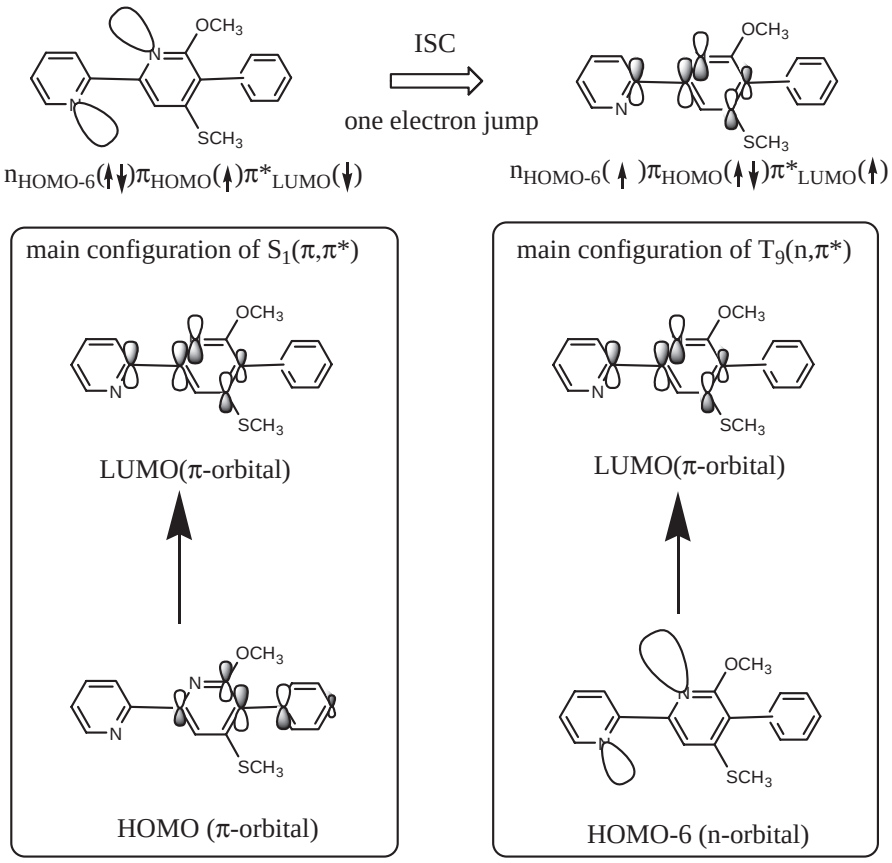

Fig. 7. Schematic explanation of $S_1(\pi, \pi^*) \rightarrow T_9(n, \pi^*)$ ISC process in case of **5a**.

In order to give a decisive answer to the drastic differences in their fluorescent intensities, we have to consider several other radiationless decay process: Pseudo-Jahn–Teller (PJT) effects[28] which play a essential role in the case of rigid aromatic hydrocarbons, the conical intersections (CI)[29] which can provide ultra-fast radiationless decay path and are widely seen for non-rigid molecules with single-bonded chromophores such as unsymmetric polymethine dyes. Further synthesis of fluorescent heterocycles and highly accurate ab-initio quantitative calculations will be reported in due course.

Experimental

The identification of compounds and measurement of the properties were carried out by general procedures using the following equipment. All melting points were determined in a capillary tube and are uncorrected. Infrared (IR) spectra were recorded in potassium bromide pellets on JASCO 810 or Shimadzu IR-460 spectrometers and ultraviolet (UV) absorption spectra were determined in 95% ethanol on a Hitachi 323 spectrometer. Fluorescence spectra were determined on a Shimadzu RF-1500. Nuclear magnetic resonance (NMR) spectra were obtained on Gemini 300NMR (300 MHz) and 500NMR (500 MHz) spectrometers with tetramethylsilane as an internal standard. Mass spectra (MS) were recorded on a JEOL DX-303 mass spectrometer. Microanalyses were performed on a Perkin-Elmer Model 2002. All chemicals were reagent grade and used without further purification unless otherwise specified.

Crystallographic data have been deposited with Cambridge Crystallographic Data Centre: Deposition numbers CCDC-290595, 290596, and 290597 for compound No. **5a**, **7a**, and **7f**, respectively. Copies of the data can be obtained free of charge via http://www.ccdc.cam.ac.uk/conts/retrieving.html (or from the Cambridge Crystallographic Data Centre, 12, Union Road, Cambridge, CB2 1EZ, UK; Fax: +44 1223 336033; e-mail: deposit@ccdc.cam.ac.uk).

Method of Fluorescence Measurement. In the Powdered State: A powder sample of subject compound was loaded onto the tray. After covering the sample with a quartz plate, this assembly was fixed in the fluorescence spectrometer. After fixing the fluorescent wavelength, the excitation spectrum was determined by scanning with the fluorescent wavelength. Similarly, the fluorescent spectrum was obtained after scanning with the excitation wavelength. After obtaining these results, the excitation wavelength was decided and the fluorescence spectrum was measured. The fluorescent relative intensity was determined by using Alq3 as a standard sample. The fluorescence of the standard sample and all subject compounds were measured upon 272 nm excitation.

In Ethanol: The fluorescence quantum yield was required as a relative fluorescence quantum yield in the comparison with 9,10-diphenylanthracene and anthracene as standard samples. The concentration of the measuring samples in the excitation wavelength region was adjusted to under 0.05 on the molar absorptivity. The fluorescence spectra in solution were obtained in a manner similar to that described for measurement in the solid state. In the case of measurement, the quantum yields of 9,10-diphenylanthracene and anthracene used were $\phi = 0.81$ and $\phi = 0.25$ under measurement at 366 and 254 nm excitation, respectively.

4-Methylthio-5-phenyl-6-oxo-1*H*-2,2′-bipyridyl (4a). Powdered sodium hydroxide (0.40 g, 10.0 mmol) was added to a solution of 1.13 g (5.0 mmol) of **1** and 0.70 g (6.0 mmol) of **2a** in 50 mL of dimethyl sulfoxide (DMSO), and the mixture was stirred for 2 h at room temperature. The reaction mixture was poured into 300 mL of ice water and neutralized with a 10% hydrochloric acid solution. The mixture was extracted with 100 mL of dichloromethane three times. The organic layer was washed with water and dried over anhydrous sodium sulfate. Removal of the solvent by evaporation gave a brown residue. A mixture of the residue and a 1% hydrochloric acid solution was refluxed for 1 h. After evaporation of the water, the residue was recrystallized from methanol to give **4a** (0.68 g, 2.31 mmol) as pale yellow crystals, in 46% yields. mp 281–283 °C. IR (potassium bromide) ν cm^{-1}: 3370 (NH or OH, broad), 1695, 1610, 1550, 1510, 1460, 1420, 1065; UV (ethanol) λ_{max} nm (log ε): 237 (4.06), 262 (4.22), 354 (4.07). ^{1}H NMR (deuteriochloroform) δ 2.46 (3H, s, SMe), 6.85 (1H, s, 3-H), 7.34–7.50 (6H, m, phenyl-H, 5″-H), 7.83 (1H, ddd, J = 1.7, 8.0, 8.0 Hz, 4″-H), 7.90 (1H, d, J = 8.0 Hz, 3″-H), 8.68 (1H, nd, J = 5.0 Hz, 6″-H), 10.61 (1H, brs, NH); Ms m/z: 295 (M$^+$ + 1, 3), 294 (M$^+$, 13), 248 (20), 247 (100), 140 (8), 106 (10), 79 (8), 78 (43), 51 (7), 44 (6). Anal. Calcd for $C_{17}H_{14}N_2OS$ = 294.372: C, 69.36; H, 4.79; N, 9.52%. Found: C, 69.37; H, 4.29; N, 9.35%.

5-(4-Methoxyphenyl)-4-methylthio-6-oxo-1*H*-2,2′-bipyridyl (4b). This compound (1.01 g, 3.12 mmol) was prepared in 62% yield from 1.13 g (5.0 mmol) of **1** and 0.88 g (6.0 mmol) of **2b** in a manner similar to that described for the synthesis of **4a**. An analytical sample was recrystallized from methanol to give yellow leaflets, mp 260–261 °C. IR (potassium bromide) ν cm^{-1}: 1605, 1510, 1275, 1250, 1175; UV (ethanol) λ_{max} nm (log ε): 263 (4.31), 356 (4.18). ^{1}H NMR (deuteriochloroform) δ 2.48 (3H, s, SMe), 3.80 (3H, s, OMe), 6.96 (2H, d, J = 8.8 Hz, phenyl-3′,5′-H), 7.22 (2H, d, J = 8.8 Hz, phenyl-2′,6′-H), 7.50 (1H, ddd, J = 1.7, 4.9, 7.5 Hz, 5″-H), 7.98 (1H, ddd, J = 1.7, 7.5, 7.7 Hz, 4″-H), 8.26 (1H, nd, J = 7.7 Hz, 3″-H), 8.28 (1H, s, 3-H), 8.71 (1H, ddd, J = 0.8, 1.7, 4.9 Hz, 6″-H), 10.99 (1H, brs, NH); Ms m/z: 325 (M$^+$ + 1, 12), 324 (M$^+$, 36), 310 (11), 309 (42), 294 (7), 278 (10), 149 (11), 84 (19), 66 (21), 57 (11), 44 (100). Anal. Calcd for $C_{18}H_{16}N_2O_2S$: C, 66.64; H, 4.97; N, 8.64%. Found: C, 66.51; H, 5.07; N, 8.51%.

5-(3,4-Dimethoxyphenyl)-4-methylthio-6-oxo-1*H*-2,2′-bipyridyl (4c). This compound (1.19 g, 3.36 mmol) was prepared in 67% yield from 1.13 g (5.0 mmol) of **1** and 0.88 g (6.0 mmol) of **2c** in a manner similar to that described for the synthesis of **4a**. An analytical sample was recrystallized from methanol to give yellow needles, mp 214–216 °C. IR (potassium bromide) ν cm^{-1}: 3010, 2930, 1710, 1620, 1580, 1500, 1460, 1315, 1250, 1225, 1170, 1140, 1070, 1050, 1030; UV (ethanol) λ_{max} nm (log ε): 258 (4.30), 307 (4.18), 369 (4.14). ^{1}H NMR (DMSO-d_6) δ 2.49 (3H, s, SMe), 3.72 (3H, s, OMe), 3.78 (3H, s, OMe), 6.80 (1H, dd, J = 1.8, 8.2 Hz, 2′-H), 6.84 (1H, d, J = 1.8 Hz, 2′-H), 6.98 (1H, d, J = 8.2 Hz, 5′-H), 7.17 (1H, brs, 3-H), 7.51 (1H, ddd, J = 2.3, 7.5, 7.9 Hz, 5″-H), 7.98 (1H, ddd, J = 1.8, 7.5, 7.9 Hz, 4″-H), 8.25 (1H, d, J = 7.9 Hz, 3″-H), 8.71 (1H, d, J = 4.1 Hz, 6″-H), 11.05 (1H, brs, NH). Ms m/z: 355 (M$^+$ + 1, 22), 354 (M$^+$, 100), 341 (6), 339 (76), 323 (13), 309 (10). Anal. Calcd for $C_{19}H_{18}N_2O_3S$ = 354.1038: C, 64.39; H, 5.12; N, 7.90%. Found: C, 64.33; H, 5.24; N, 7.87%.

6-Methoxy-4-methylthio-5-phenyl-2,2′-bipyridyl (5a). Powdered sodium hydroxide (0.40 g, 10.0 mmol) was added to a solution of 1.13 g (5.0 mmol) of **1** and 0.70 g (6.0 mmol) of **2a** in 50 mL of dimethyl sulfoxide (DMSO), and the mixture was stirred for 2 h at room temperature. The reaction mixture was poured into 300 mL of ice water and neutralized with a 10% hydrochloric acid solution. The mixture was extracted with 100 mL of dichloromethane three times. The organic layer was washed with water and dried over anhydrous sodium sulfate. Removal of the solvent by evaporation gave a brown residue. A solution of the residue in 100 mL of methanol was refluxed for 6 h. After the reaction, evaporation of the solvents under reduced pressure gave a tan solid, which was crystallized by the addition of 10 mL of methanol. The product was collected by filtration and recrystallized from methanol to give 0.83 g (2.69 mmol, 54%) of **5a** as yellow needles; mp 154–156 °C. IR (potassium bromide) ν cm^{-1}: 1580, 1540, 1425, 1355, 1280, 1040; UV (ethanol) λ_{max} nm (log ε): 246 (4.51), 307 (4.34). ^{1}H NMR (deuteriochloroform) δ 2.56 (3H, s, SMe), 4.02 (3H, s, OMe), 7.38–7.55 (5H, m, phenyl-H), 7.38 (1H, ddd, J = 1.2, 4.8, 6.3 Hz, 5″-H), 7.87 (1H, ddd, J = 1.6, 6.3, 8.0 Hz, 4″-H), 8.08 (1H, s, 3-H), 8.50 (1H, ddd, J = 0.8, 1.2, 8.0 Hz, 3″-H), 8.72 (1H, ddd, J = 0.8, 1.6, 4.8 Hz, 6″-H); Ms m/z: 309 (M$^+$ + 1, 23), 308 (M$^+$, 100), 307 (54), 293 (28), 263 (15), 261 (13), 146 (10), 81 (16), 69 (32), 57 (13), 55 (14), 44 (10). Anal. Calcd for $C_{18}H_{16}N_2OS$: C, 70.10; H, 5.23; N, 9.08%. Found: C, 70.05; H, 5.27; N, 9.07%.

6-Methoxy-5-(4-methoxyphenyl)-4-methylthio-2,2′-bipyridyl (5b). This compound (0.57 g, 1.7 mmol) was prepared in 34% yield from 1.13 g (5.0 mmol) of **1** and 0.88 g (6.0 mmol) of **2b** in a manner similar to that described for the synthesis of **5a**. An analytical sample was recrystallized from methanol to give yellow leaflets, mp 179–180 °C. IR (potassium bromide) ν cm^{-1}: 3425, 2940, 1610, 1570, 1540, 1510, 1450, 1430, 1350, 1270, 1250, 1170, 1105, 1035; UV (ethanol) λ_{max} nm (log ε): 247 (4.48), 309 (4.35). ^{1}H NMR (deuteriochloroform) δ 2.52 (3H, s, SMe), 3.86 (3H, s, OMe), 3.98 (3H, s, OMe), 7.00 (2H, d, J = 8.8 Hz, 3′,5′-H), 7.29 (2H, d, J = 8.8 Hz, 2′,6′-H), 7.30 (1H, ddd, J = 1.2, 4.8, 6.3 Hz, 5″-H), 7.82 (1H, ddd, J = 1.6, 6.3, 7.9 Hz, 4″-H), 8.01 (1H, s, 3-H), 8.45 (1H, ddd, J = 0.8, 1.2, 7.9 Hz, 3″-H), 8.68 (1H, ddd, J = 0.8, 1.6, 4.8 Hz, 6″-H); Ms m/z: 339 (M$^+$ + 1, 24), 338 (M$^+$, 100), 337 (29), 323 (19), 293 (8), 291 (7), 161 (6), 121 (5), 105 (5), 78 (5), 44 (4). Anal. Calcd for $C_{19}H_{18}N_2SO_2$: C, 67.43; H, 5.36; N, 8.28%. Found: C, 67.61; H, 5.50; N, 8.10%.

5-(3,4-Dimethoxyphenyl)-6-methoxy-4-methylthio-2,2′-bipyridyl (5c). This compound (0.75 g, 2.1 mmol) was prepared in 41% yield from 1.13 g (5.0 mmol) of **1** and 0.88 g (6.0 mmol) of **2c** in a manner similar to that described for the synthesis of **5a**. An analytical sample was recrystallized from methanol to give yellow prisms, mp 165–167 °C. IR (potassium bromide) ν cm^{-1}: 3450, 2940, 1580, 1540, 1515, 1450, 1430, 1350, 1250, 1210, 1170, 1140, 1030; UV (ethanol) λ_{max} nm (log ε): 246 (4.52), 310 (4.32); ^{1}H NMR (deuteriochloroform) δ 2.52 (3H, s, SMe), 3.90 (3H, s, OMe), 3.93 (3H, s, OMe), 4.00 (3H, s, pyridyl-OMe), 6.88 (1H, d, J = 1.8 Hz, 2′-H), 6.92 (1H, dd, J = 1.8, 8.3 Hz, 6′-H), 6.98 (1H, d, J = 8.3 Hz, 5′-H), 7.31 (1H, m, 5″-H), 7.82 (1H, ddd, J = 1.8, 7.7, 7.9 Hz, 4″-H), 8.02 (1H, s, 3-H), 8.45 (1H, d, J = 7.9 Hz, 3″-H), 8.67 (1H, m, 6″-H); Ms m/z: 369 (M$^+$ + 1, 6), 368 (M$^+$, 25), 279 (25), 179 (12), 178 (100), 167 (25), 149 (54), 147 (10), 106 (25), 78 (37), 75 (10), 71 (13), 70 (11), 69 (15), 57 (21), 55 (11), 44 (17), 43 (16). Anal. Calcd for $C_{20}H_{20}N_2SO_3$: C, 65.20; H, 5.47; N, 7.60%. Found: C, 65.37; H, 5.48; N, 7.47%.

4-Methylthio-5-phenyl-6-(1-pyrrolidinyl)-2,2′-bipyridyl (7a). Powdered sodium hydroxide (0.40 g, 10.0 mmol) was added to a solution of 1.13 g (5.0 mmol) of **1** and 0.70 g (6.0 mmol) of **2a** in 50 mL of DMSO, and the mixture was stirred for 2 h at room temperature. The reaction mixture was poured into 300 mL of

ice water and neutralized with a 10% hydrochloric acid solution. The mixture was extracted with 100 mL of dichloromethane three times. The organic layer was washed with water and dried over anhydrous sodium sulfate. Removal of the solvent by evaporation gave a brown residue. A mixture of the residue and 1.42 g (20 mmol) of pyrrolidine was refluxed for 6 h. After evaporation of the excess pyrrolidine, the residue was chromatographed on an alumina column by using toluene as an eluent to give 0.87 g (2.51 mmol, 50%) of **7a**. This compound was recrystallized from methanol to give colorless needles. mp 157–158 °C. IR (potassium bromide) ν cm^{-1}: 2975, 2920, 2850, 1610, 1570, 1530, 1430, 1415; UV (ethanol) λ_{max} nm (log ε): 255 (4.58), 355 (4.06); ^{1}H NMR (deuteriochloroform) δ 1.73 (4H, m, pyrrolidino 3,4-H), 2.47 (3H, s, SMe), 3.16 (4H, m, pyrrolidino 2,5-H), 7.25–7.31 (1H, m, 3″-H), 7.34–7.56 (5H, m, phenyl-H), 7.74 (1H, s, 3-H), 7.80 (1H, ddd, J = 2.0, 8.0, 8.2 Hz, 4″-H), 8.46 (1H, d, J = 8.2 Hz, 5″-H), 8.65 (1H, m, 6″-H); Ms m/z: 348 ($M^+ + 1$, 28), 347 (M^+, 100), 346 (54), 319 (43), 318 (70), 304 (27), 292 (12), 264 (12), 263 (57), 231 (10), 153 (15), 152 (13), 97 (10), 85 (15), 83 (13), 78 (22), 71 (18), 70 (17), 69 (16), 57 (30), 44 (47). Anal. Calcd for $C_{21}H_{21}N_3S$: C, 72.59; H, 6.09; N, 12.09%. Found: C, 72.18; H, 6.11; N, 11.95%.

6-Amino-4-methylthio-5-phenyl-2,2′-bipyridyl (7b). Powdered sodium hydroxide (0.4 g, 10 mmol) was added to a solution of 1.13 g (5.0 mmol) of **1** and 0.70 g (6.0 mmol) of **2a** in 50 mL of DMSO, and the mixture was stirred for 4 h at room temperature. The reaction mixture was poured into 300 mL of ice-water and neutralized with a 10% hydrochloric acid solution. The mixture was extracted with 100 mL of dichloromethane three times. The organic layer was washed with 200 mL of water and dried over anhydrous magnesium sulfate. Removal of the solvent by evaporation gave a brown residue. A mixture of this residue and 150 mL of 28% aqueous ammonia was refluxed for 2 h. After evaporation of ammonia and water, the residue was chromatographed on a silica-gel column by using toluene as an eluent to give 0.441 g (1.51 mmol, 30%) of **7b** as colorless needles. This product was recrystallized from methanol to give colorless prisms, mp 117–120 °C. IR (potassium bromide) ν cm^{-1}: 3440, 3270, 3160 (NH_2), 1620, 1535, 1415, 700; UV (ethanol) λ_{max} nm (log ε): 248 (4.56), 330 (4.23). ^{1}H NMR (deuteriochloroform) δ 2.40 (3H, s, SMe), 4.25 (2H, brs, NH_2), 7.24 (1H, m, 5″-H), 7.28 (2H, m, phenyl-H), 7.37–7.47 (3H, m, phenyl-H), 7.67 (1H, s, 3-H), 7.72 (1H, ddd, J = 2.2, 7.9, 8.0 Hz, 4″-H), 8.24 (1H, d, J = 7.9 Hz, 3″-H), 8.59 (1H, m, 6″-H); Ms m/z: 294 ($M^+ + 1$, 25), 293 (M^+, 100), 292 (76), 278 (22), 260 (16), 246 (21). HYRMS: Calcd for $C_{17}H_{15}N_3S$ = 293.0962; Found: 293.0987. Anal. Calcd for $C_{17}H_{15}N_3S$: C, 69.59; H, 5.15; N, 14.32%. Found: C, 69.33; H, 5.04; N, 14.48%.

6-Amino-5-(4-methoxyphenyl)-4-methylthio-2,2′-bipyridyl (7c). This compound (0.65 g, 2.0 mmol) was prepared in 40% yield from 1.13 g (5.0 mmol) of **1** and 0.88 g (6.0 mmol) of **2b** in a manner similar to that described for the synthesis of **7b**. An analytical sample was recrystallized from methanol to give yellow needles, mp 233–235 °C. IR (potassium bromide) ν cm^{-1}: 2950, 1615, 1580, 1520, 1465, 1430, 1340, 1290, 1250, 1185, 1165, 1120, 1030, 1000; UV (ethanol) λ_{max} nm (log ε): 343 (4.24); ^{1}H NMR (deuteriochloroform) δ 2.46 (3H, s, SMe), 3.85 (3H, s, OMe), 4.33 (1H, brs, NH), 7.00 (2H, d, J = 8.8 Hz, 3′,5′-H), 7.31–7.40 (1H, m, 5″-H), 7.35 (2H, d, J = 8.8 Hz, 2′,6′-H), 7.73 (1H, s, 3-H), 7.77–7.88 (1H, m, 4″-H), 8.31 (1H, d, J = 8.0 Hz, 3″-H), 8.66–8.68 (1H, m, 6″-H), 10.56 (1H, s, NH); MS m/z: 325 ($M^+ + 2$, 8), 324 ($M^+ + 1$, 25), 323 (M^+, 100), 322 (58), 308 (21), 276 (10), 44 (5). HYRMS: $C_{18}H_{17}N_3OS$ = 323.1092, Found: 323.1117.

6-Dimethylamino-5-(4-methoxyphenyl)-4-methylthio-2,2′-bipyridyl (7d). This compound (1.05 g, 3.0 mmol) was prepared in 60% yield from 1.13 g (5.0 mmol) of **1** and 0.88 g (6.0 mmol) of **2b**, and 2 mL of a 50% dimethylamine solution in a manner similar to that described for the synthesis of **7a**. An analytical sample was recrystallized from methanol to give yellow needles, mp 164–165 °C. IR (potassium bromide) ν cm^{-1}: 2975, 2855, 1550, 1520, 1435, 1385, 1300, 1260; UV (ethanol) λ_{max} nm (log ε): 254 (4.51), 349 (4.10); ^{1}H NMR (deuteriochloroform) δ 2.48 (3H, s, SMe), 2.72 (6H, s, NMe2), 3.87 (3H, s, OMe), 6.99 (2H, d, J = 8.2 Hz, 3′,5′-H), 7.28 (1H, d, J = 7.4 Hz, 5″-H), 7.29 (2H, d, J = 8.2 Hz, 2′,6′-H), 7.80 (1H, m, 4″-H), 7.86 (1H, s, 3-H), 8.45 (1H, dd, J = 0.8, 7.1 Hz, 3″-H), 8.65 (1H, m, 6″-H); Ms m/z: 352 ($M^+ + 1$, 23), 351 (M^+, 79), 350 (73), 338 (11), 337 (12), 336 (34), 321 (11), 305 (10), 304 (14), 293 (15), 69 (20), 44 (100). Anal. Calcd for $C_{20}H_{21}N_3OS$: C, 68.35; H, 6.02; N, 11.96%. Found: C, 68.50; H, 6.05; N, 11.93%.

5-(4-Methoxyphenyl)-4-methylthio-6-(1-pyrrolidinyl)-2,2′-bipyridyl (7e). This compound (1.23 g, 2.3 mmol) was prepared in 65% yield from 1.13 g (5.0 mmol) of **1**, 0.88 g (6.0 mmol) of **2b**, and 1.42 g (20 mmol) of pyrrolidine in a manner similar to that described for the synthesis of **7a**. An analytical sample was recrystallized from methanol to give yellow leaflets, mp 167–168 °C. IR (potassium bromide) ν cm^{-1}: 2975, 2855, 1550, 1450, 1435, 1255; UV (ethanol) λ_{max} nm (log ε): 228 (4.79), 256 (4.84), 270 (4.82), 357 (4.27); ^{1}H NMR (deuteriochloroform) δ 1.74 (4H, s, pyrrolidino 3,4-H), 2.47 (3H, s, SMe), 3.17 (4H, s, pyrrolidino 2,5-H), 3.86 (3H, s, OMe), 6.95 (2H, d, J = 8.8 Hz, 3′,5′-H), 7.23–7.29 (1H, m, 5″-H), 7.25 (2H, d, J = 8.8 Hz, 2′,6′-H), 7.72 (1H, s, 3-H), 7.79 (1H, ddd, J = 2.0, 8.0, 8.0 Hz, 4″-H), 8.45 (1H, d, J = 8.0 Hz, 3″-H), 8.65 (1H, m, 6″-H); Ms m/z: 378 ($M^+ + 1$, 30), 377 (M^+, 100), 376 (70), 349 (38), 348 (62), 334 (34), 294 (11), 293 (45), 164 (10), 78 (12), 44 (50). Anal. Calcd for $C_{22}H_{23}N_3OS$: C, 70.00; H, 6.14; N, 11.13%. Found: C, 69.74; H, 6.15; N, 11.10%.

5-(3,4-Dimethoxyphenyl)-4-methylthio-6-(1-pyrrolidinyl)-2,2′-bipyridyl (7f). This compound (1.23 g, 2.3 mmol) was prepared in 74% yield from 1.13 g (5.0 mmol) of **1**, 0.88 g (6.0 mmol) of **2c**, and 1.42 g (20 mmol) of pyrrolidine in a manner similar to that described for the synthesis of **7a**. An analytical sample was recrystallized from methanol to give yellow leaflets, mp 166–168 °C. IR (potassium bromide) ν cm^{-1}: 2975, 2950, 2860, 1595, 1550, 1520, 1475, 1435, 1275, 1260; UV (ethanol) λ_{max} nm (log ε): 232 (4.53), 256 (4.56), 269 (4.55), 351 (3.00), 358 (4.03). ^{1}H NMR (deuteriochloroform) δ 1.74 (4H, s, pyrrolidino 3,4-H), 2.48 (3H, s, SMe), 3.19 (4H, s, pyrrolidino 2,5-H), 3.88 (3H, s, OMe), 3.94 (3H, s, OMe), 6.87 (1H, d, J = 11.0 Hz, 5′-H), 6.89 (1H, d, J = 11.0 Hz, 6′-H), 6.91 (1H, s, 2′-H), 7.27 (1H, m, 5″-H), 7.73 (1H, s, 3-H), 7.79 (1H, ddd, J = 1.6, 8.0, 8.0 Hz, 4″-H), 8.45 (1H, dd, J = 0.8, 8.0 Hz, 3″-H), 8.66 (1H, m, 6″-H); Ms m/z: 408 ($M^+ + 1$, 28), 407 (M^+, 100), 406 (41), 392 (71), 378 (40), 364 (25), 323 (30), 307 (11), 97 (14), 95 (11), 85 (17), 83 (17), 81 (10), 71 (24), 70 (17), 69 (26), 57 (41), 44 (35), 43 (38). Anal. Calcd for $C_{23}H_{25}N_3O_2S$: C, 67.79; H, 6.18; N, 10.31%. Found: C, 67.73; H, 6.19; N, 10.29%.

This work was in part financially supported by Shiseido Inc. Science grand 2003. The financial assistance from Canon Inc. is also acknowledged in performing quantum chemical calculations.

Supporting Information

The $S_1 \rightarrow S_0$ vertical transition energies calculated using the semiempirical ZINDO method are described in Supporting Information. This material is available free of charge on the web at http://www.csj.jp/journals/bcsj/.

References

1 J. Wilson, J. F. Hawkes, *Optopelectronics: An Introduction*, 3rd ed., Prentice Hall, **1998**.

2 Y. Iwasaki, M. Matsumura, *Kagaku (Chemistry)* **2005**, *60*, 29.

3 H. Zollinger, *Color Chemistry*, 2nd ed., VCH Publishers, Weinheim, **1991**.

4 a) *Colour Chemistry: The Design and Synthesis of Organic Dyes and Pigments (Advances in Colour Chemistry Series)*, ed. by A. T. Peters, H. S. Freeman, Elsevier Application Science, New York, **1991**. b) *The Chemistry and Application of Dyes*, ed. by D. R. Waring, G. Hallas, Plenum Press, New York, **1991**. c) D. M. Sturmer, *Chem. Heterocycl. Compd.* **1977**, *30*, 441. d) J. Fabian, H. Nakazumi, M. Matsuoka, *Chem. Rev.* **1992**, *92*, 1197. e) J. Griffiths, *Colour and Constitution of Organic Molecules*, Academic Press, London, **1976**. f) J. Fabian, H. Hartmann, *Light Absorption of Organic Colorants*, Springer-Verlag, Berlin, **1980**.

5 J.-Y. Jaung, M. Matsuoka, K. Fukunishi, *Dyes Pigm.* **1998**, *37*, 135.

6 K. Shirai, A. Yanagisawa, H. Takahashi, K. Fukunishi, M. Matsuoka, *Dyes Pigm.* **1998**, *39*, 49.

7 K. Shirai, M. Matsuoka, K. Fukunishi, *Dyes Pigm.* **2000**, *47*, 107.

8 M. Belletete, M. Bedrard, M. Leclerc, G. Durocher, *THEOCHEM* **2004**, *679*, 9.

9 a) K. Hirano, S. Minakata, M. Komatsu, *Chem. Lett.* **2000**, 8. b) K. Hirano, S. Minakata, M. Komatsu, *Bull. Chem. Soc. Jpn.* **2001**, *74*, 1567.

10 K. Tanaka, T. Miura, N. Umezawa, Y. Urano, K. Kikuchi, T. Higuchi, T. Nagano, *J. Am. Chem. Soc.* **2001**, *123*, 2530.

11 R. J. Cave, K. Burke, E. W. Castner, Jr., *J. Phys. Chem. A* **2002**, *106*, 9294.

12 L. Serrano-Andres, M. Merchan, B. O. Roos, R. Lindh, *J. Am. Chem. Soc.* **1995**, *117*, 3189.

13 F. Fratev, G. Hiebaum, A. Gochev, *J. Mol. Struct.* **1974**, *23*, 437.

14 W. Fabian, *Dyes Pigm.* **1985**, *6*, 341.

15 a) C. Kaes, A. Katz, M. W. Hosseini, *Chem. Rev.* **2000**, *100*, 3553. b) G. Celucci, P. P. Thummel, *Chem. Rev.* **2002**, *102*, 3129.

16 a) K. Araki, T. Mutai, Y. Shigemitsu, M. Yamada, T. Nakajima, S. Kuroda, I. Shimazu, *J. Chem. Soc., Perkin Trans. 2* **1996**, 613. b) C.-S. Choi, L. Mishra, T. Mutai, K. Araki, *Bull. Chem. Soc. Jpn.* **2000**, *73*, 2051.

17 K. T. Potts, M. J. Cipullo, P. Ralli, G. Theodoridis, *J. Org. Chem.* **1982**, *47*, 3027.

18 a) Y. Tominaga, N. Yoshioka, S. Kataoka, *Heterocycles* **1996**, *43*, 1597. b) Y. Tominaga, N. Yoshioka, H. Minematsu, S. Kataoka, *Heterocycles* **1996**, *44*, 85. c) Y. Tominaga, A. Ushirogouchi, Y. Matsuda, G. Kobayashi, *Chem. Pharm. Bull.* **1984**, *32*, 3384.

19 *Cache WorkSystem Version 5.04*, Fujitsu Ltd., **2002**.

20 J. S. Dewar, E. G. Zoebisch, E. G. Hearly, J. J. P. Stewart, *J. Am. Chem. Soc.* **1985**, *107*, 3902.

21 a) T. A. Engeland, T. Bultmann, N. P. Ernsting, M. A. Rodriguez, W. Thiel, *Chem. Phys.* **1992**, *163*, 43. b) S. Mitra, R. Das, S. P. Bhattacharyya, S. Mukherjee, *J. Phys. Chem. A* **1997**, *101*, 293. c) P. Purkayastha, P. K. Bhattacharyya, S. C. Bera, N. Chattopadlhyav, *Phys. Chem. Chem. Phys.* **1999**, *1*, 3253.

22 A. Broo, *J. Phys. Chem. A* **1998**, *102*, 526.

23 A. B. J. Parusel, W. Rettig, W. Sudholt, *J. Phys. Chem. A* **2002**, *106*, 804.

24 J. Ridley, M. C. Zener, *Theor. Chim. Acta* **1973**, *32*, 111.

25 a) M. A. El-Sayed, *J. Chem. Phys.* **1963**, *38*, 2834. b) K. Klessinger, J. Michl, *Excited State and Photochemistry of Organic Molecules*, VCH Publishers, New York, **1995**.

26 N. J. Turro, *Modern Molecular Photochemistry*, University Science Book, **1991**.

27 a) J. T. Dubois, F. Wilkinson, *J. Chem. Phys.* **1963**, *39*, 899. b) P. Avouris, W. M. Gelbart, M. A. El-Sayed, *Chem. Rev.* **1977**, *77*, 793.

28 a) W. A. Wassam, Jr., E. C. Lim, *J. Chem. Phys.* **1978**, *68*, 433. b) E. C. Lim, *J. Phys. Chem.* **1986**, *90*, 6770.

29 M. Dekhtyar, W. Rettig, M. Sczepan, *Phys. Chem. Chem. Phys.* **2000**, *2*, 1129.